SUPPLEMENTAL METHODS

Criteria for selection of representative STAT3 mutations for examination. All STAT3 mutations studied cause either AD-HIES or cancer and were selected, in part, based on their identification in patients with these diseases in previous publications (**Supplemental Table 1**). In addition, we previously classified STAT3 LOF mutations as either structural, functional, or structural/functional. STAT3 LOF mutation, R382W in the DBD was classified as a functional mutation[1], since the side chain of R382, but not W382, can form a salt bridge with DNA (**Supplemental Figure 11A**). Also, our computer-based structural analysis of STAT3-R382W predicted that this mutation has minimal impact on the structure of the DBD.[1] DBD residues predicted computationally to have a structural role that is supported by X-ray crystallographic data of STAT3 homodimer bound to DNA (PDB: 1bg1) include residues F384, H437 and V463, which were found to have no direct contact with DNA. Rather, they engaged in crucial intramolecular contacts that define the architecture of the DBD (**Supplemental Figure 11A**); mutations at these residues are likely to have a disruptive impact on the folding and stability of STAT3.[1] STAT3 LOF mutations in the SH2D at residues S636 and S668 are examples of mutations that were classified as functional mutations because these residues were predicted to be directly involved in binding of the phosphotyrosine (pY705) peptide ligand within the Loop region. Mutations at V637 were classified as structural-functional, since, in addition to direct interactions with the pY705-peptide ligand, the side chain of V637 is buried and contributes to critical hydrophobic interactions that stabilize the SH2D structure. Mutations at residue N647 were classified as structural-functional[1], since this residue was predicted to have a structural role as well as being the only STAT3 residue that forms intermolecular polar interactions with its amino acid counterpart in the homodimer partner (**Supplemental Figure 11B and C**). Mutations of residues T622 and Y657 were classified as structural[1], since they were predicted to have only a structural role (**Supplemental Figure 11C**).

DNA constructs for BRET assay. To generate NanoLuc-STAT3 WT (NS), we amplified the cDNA of NanoLuc luciferase from pNL1.1.PGK[Nluc/PGK] vector and inserted it by overlap extension PCR cloning

at the N-terminus of STAT3 sequence within the expression vector EX-Z2835-M02 (Genecopoea). The insertion was confirmed by DNA sequencing. To generate NLuc–STAT3 WT–FlAsH (NSF), we inserted the CCPGCC amino acid motif into NS within loop domains of STAT3 located at amino acid residue positions 225, 425, 535 and 688 using overlap extension PCR[2]. After testing and validation, insertion of the CCPGCC motif at position 425 was determined to be the most sensitive reporter of conformational changes in STAT3 after IL6 treatment. We generated LOF and GOF mutant NSF constructs from the NLuc-STAT3 WT–FlAsH construct using QuikChange II XL Site-Directed Mutagenesis. Each construct was verified by DNA sequencing. All information about DNA primers used is provided in **Supplemental Table 2**.

BRET Assay. STAT3$^{-/-}$ MEF cells were seeded in 6-well plates and transfected, as described in the materials and methods section. After 4 hours at 37˚ C, the cells were trypsinized and re-plated (30,000cells/well) in white-wall clear-bottom 96-well plates and left to adhere and grow for 48 hours at 37˚ C / 5% CO_2. The cells were then labeled with a FlAsH probe using a TC-FlAsH™ II In-Cell Tetracysteine Tag Detection Kit. (ThermoFisher Scientific). Briefly, cells were washed with PBS three times. FlAsH-EDT2 was diluted in HBSS containing calcium and magnesium to a final concentration of 1.25uM and incubated with the cells for 60 minutes. Then, the cells were washed with BAL wash buffer three times and incubated at 37˚C in DMEM complete media with 10% FBS for at least 1 h, after which the cells were washed with HBSS containing calcium and magnesium and supplemented with 1X pyruvate and 1X Glutamax. Conformational changes of NLuc–STAT3–FlAsH (NSF) sensors were detected on a Synergy H1 microplate reader (BioTek Inc, VT, and USA) with 485nm excitation and 525–585nm emission filters. Measurements were initiated when coelenterazine was added at a final concentration of 5µM in the HBSS final wash media. After 5 min, cells were treated with IL6/sIL6R (@200ng/ml) and monitored at 1 min intervals for 60 min. The BRET ratio was calculated by dividing the FlAsH fluorescence signal (530 nm) by the nLuc signal (480 nm) after each were normalized by subtracting the mean of the baseline readings at each wavelength.

Phosphopeptide pull-down assay. Neutravidin agarose beads (Pierce) were blocked with 20% BSA in PBS overnight then resuspended in PBS to make a 50% slurry and aliquoted into two fractions. One fraction was spiked with pY1068 peptide and the other was spiked with biotinylated Y1068 peptide (control) to a final concentrations of 100ug/ml. After incubation for 1 hour, the beads were washed 3 times with PBS, resuspended in binding buffer (25 mM HEPES pH 7.5 containing 5% BSA, 0.05% Triton-X100), and aliquoted into 30ul fractions. Lysates were diluted 10-fold in binding buffer containing protease and phosphatase inhibitor cocktails (Roches); diluted lysate (100ul) was added to a tube containing pY1068 peptide and a corresponding tube containing Y1068 peptide (control). The samples were incubated for 1 hour at 4°C on a rotator then washed 4 times with 500 µl of wash buffer (25 mM HEPES pH 7.5 containing 5% BSA, 0.5% NP40) and resuspended in SDS-PAGE buffer prior to gel electrophoresis and immunoblotting.

Immunoblotting. Cell extracts or bead-bound proteins were denatured in SDS-PAGE buffer by heating. The samples were then separated on SDS-PAGE gels and transferred to a polyvinyldene difloride (PVDF) membrane. Protein levels were determined by probing with specific antibodies to STAT3 (9139T and 9145) purchased from Cell Signaling and beta actin (A2228) purchased from Sigma.

Recombinant STAT3 protein expression and purification. The cDNA encoding core STAT3 protein (residues 127-722) was cloned into a pET15b plasmid. To express non-phosphorylated STAT3 monomers, plasmid were transformed into *E. coli* (strain BL21 DE; Life Technologies, Inc.) cells and induced with 0.5mM IPTG at 20˚C for 5 h. To express pY-STAT3 homodimers, plasmids were transformed into BL21 *E. coli* (strain DE3; Stratagene) that expresses TANK-binding kinase 1 (TBK1). Induction and Y705 phosphorylation of STAT3 was achieved by addition of IPTG followed by addition of 3 β-indoleacrylic acid, as described[3]. After lysis of bacteria, STAT3 protein was precipitated using ammonium sulfate at 35% saturation and purified to homogeneity in two steps—a HiTrap Q column (GE Healthcare) for the monomeric STAT3 or a HiTrap heparin column (GE Healthcare) for pY-STAT3 homodimers followed by

size-exclusion chromatography. Except for mutants F384S and H437P, WT and all other mutant STAT3 constructs could be expressed in soluble form and purified to homogeneity from bacteria both as unphosphorylated monomers and as a phosphorylated homodimers. Purity of the resulting protein samples was verified by SDS PAGE and Coomassie blue staining and by gel filtration (**Supplemental Figure 4A** and **B**). Unphosphorylated and phosphorylated mutant F384S and H437P STAT3 proteins were found almost exclusively in the insoluble fraction when expressed in bacteria and, therefore, could not be purified in native form for biophysical studies.

Native polyacrylamide gel electrophoresis (PAGE). PAGE of STAT3 protein samples was performed under native conditions using the Native PAGE TM Novex Bis-Tris gel system (Invitrogen) following the manufacturer's protocol. Coomassie G250 (0.02%) was added to the cathode buffer; STAT3 samples (10ul of 5uM) were loaded into each well. Protein bands were visualized by fast Coomassie blue staining, as described by the manufacture.

Crosslinking of STAT3 proteins. Aliquots of phosphorylated or unphosphorylated WT and mutant STAT3 proteins (5uM) were incubated with 0.5 mM BS(PEG)9 (Thermo Fisher Scientific) in 20-mM HEPES, pH 7.4, 200 mM NaCl, and 5mM 2-Mercaptoethanol for 30 min at 4 °C. Protein samples were then separated by SDS-PAGE; gels were stained with the Coomassie blue dye for visualization of protein bands.

Surface plasmon resonance (SPR) assays for pY-peptide binding and for DNA binding. A Biacore 3000 instrument equipped with SA streptavidin chip was used; one of the flow cells was immobilized with biotinylated pY1068-peptide, while another (reference) flow cell was immobilized with unphosphorylated Y1068 peptide. Phosphopeptide binding was performed in 20mM HEPES buffer PH 7.5, 50mM NaCl, 0.05% Tween 20 and 1mM 2-Mercaptoethanol. Aliquots of monomeric STAT3 protein at different concentrations ranging from 0.3uM to 5uM were injected onto the chip for 3 min at a flow rate of 30uL/min.

In between each injection, the chip was regenerated with 0.1% SDS solution. Each SPR measurement was repeated three times to obtain the K_D (mean ± SD). Affinity constants for DNA binding were obtained using a similar SPR approach, except that immobilized biotinylated duplex hSIE oligonucleotide was used[4,5]. DNA-binding experiments were performed in 20mM HEPES, 100 mM NaCl, 10 mM MgCl2, and 0.05% Tween 20. Different concentrations of pY-STAT3 dimer (0.3uM to 16uM) were injected into the flow cells to generate sensograms for K_D analysis. Each concentration was run in triplicate. Chip regeneration was achieved with 0.5M $MgCl_2$ solution.

Assessment of dominant negative effect of STAT3 LOF mutant R382W. $STAT3^{-/-}$ MEF cells were transfected as described in the materials and methods section with either 3ug of WT STAT3 pAcGFP1-C1 vector, 3ug of untagged STAT3 R382W mutant in EX-Z2835-M02 vector or co-transfected with both constructs at varying amounts (ug) — WT: mutant (2:1 and 1.5:1.5), cells were incubated for 48Hrs at 37˚ C / 5% CO_2 and then treated with or without IL6/sIL6R (@100ng/ml. The lysates were then analyzed for DNA binding using the TransAM STAT3 kit following the manufacturer's protocol as described in the material and method section.

References Cited

1. Bocchini CE, Nahmod K, Katsonis P, et al. Protein stabilization improves STAT3 function in autosomal dominant hyper-IgE syndrome. *Blood*. 2016;128(26):3061-3072.
2. Bryksin AV, Matsumura I. Overlap extension PCR cloning: a simple and reliable way to create recombinant plasmids. *Biotechniques*. 2010;48(6):463-465.
3. Baudin F, Müller CW. Bacterial expression, purification, and crystallization of tyrosine phosphorylated STAT proteins. *Methods Mol Biol*. 2013;967:301-317.
4. Yu CL, Meyer DJ, Campbell GS, et al. Enhanced DNA-binding activity of a Stat3-related protein in cells transformed by the Src oncoprotein. *Science*. 1995;269(5220):81-83.
5. Minus MB, Liu W, Vohidov F, et al. Rhodium(II) Proximity-Labeling Identifies a Novel Target Site on STAT3 for Inhibitors with Potent Anti-Leukemia Activity. *Angew Chem Int Ed Engl*. 2015;54(44):13085-13089.

Supplemental Figure 1

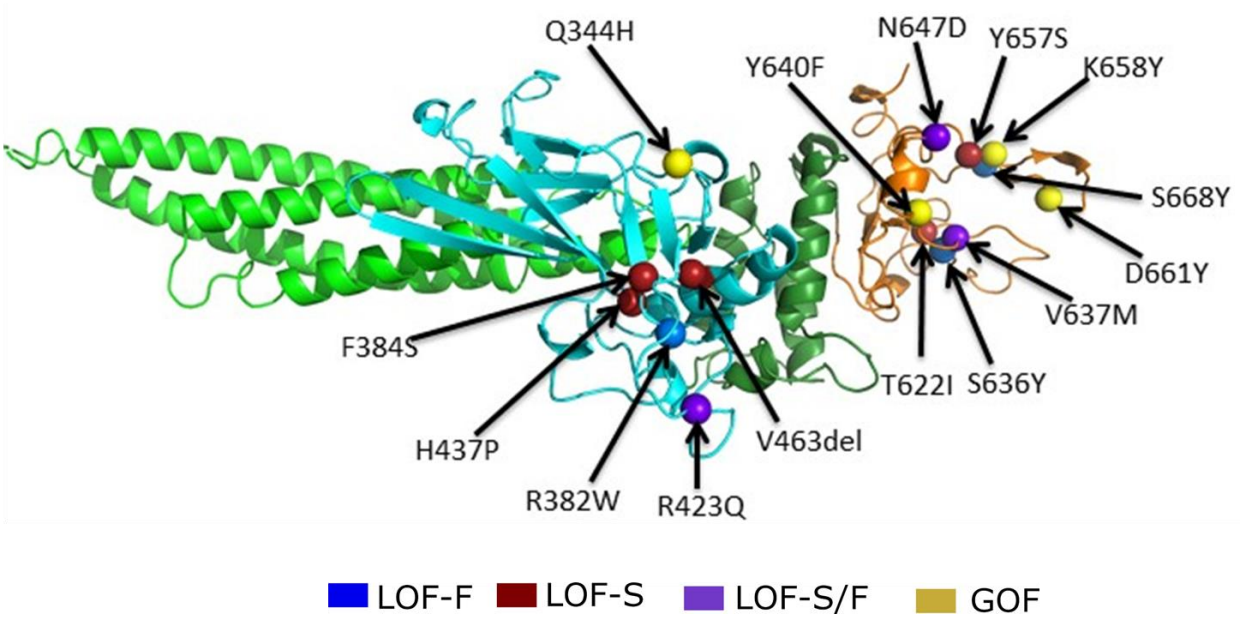

Supplemental Figure 1. **STAT3 mutations generated and examined in this study.** Ribbon diagram obtained from the three-dimensional structure of truncated human STAT3β showing each mutation color-coded based on its previous categorization as loss-of-function (LOF) or gain-of-function (GOF). The LOF mutations were further subcategorized as functional (F), structural (S), or structural and function (S/F), as described in the text.

Supplemental Figure 2

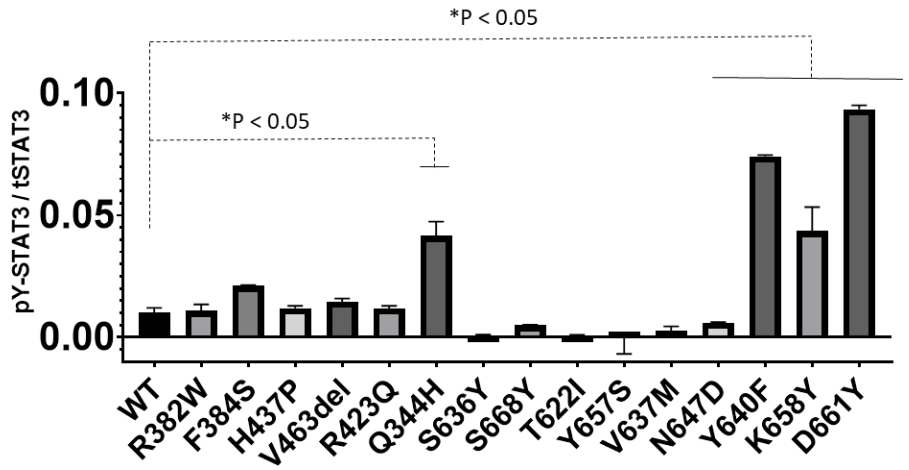

Supplemental Figure 2. Effect of mutations on basal STAT3 Y705 phosphorylation in MEF cells. The mean ± SD densitometry results of three immunoblots showing the effects of STAT3 mutations on constitutive pY-STAT3. Data was extracted from **Figure 1** (*, $p < 0.05$; Student's t-test).

Supplemental Figure 3

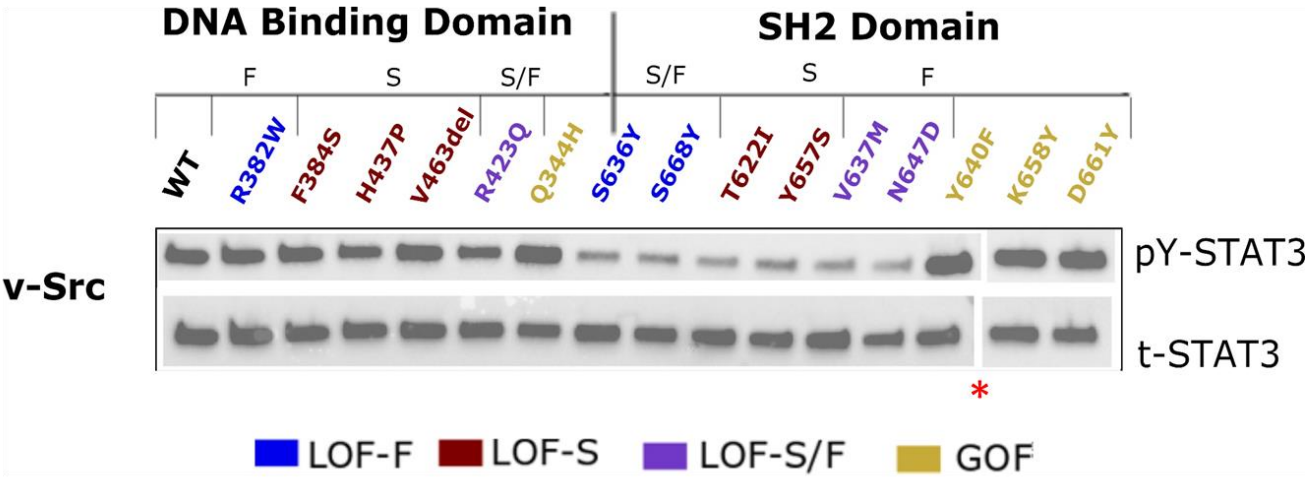

Supplemental Figure 3. Effect of mutations on v-Src-mediate STAT3 Y705 phosphorylation in MEF cells. Protein extracts of STAT3$^{-/-}$ MEF cells transiently co-transfected with v-Src and either Ac-GFP-tagged WT or mutant STAT3α expression constructs; cell lysates were immunoblotted for pY-STAT3 or total (t) STAT3. A representative of 3 immunoblots is shown. The red asterisk (*) indicates that the images are a composite of two separate blots imaged simultaneously with equal exposure.

Supplemental Figure 4

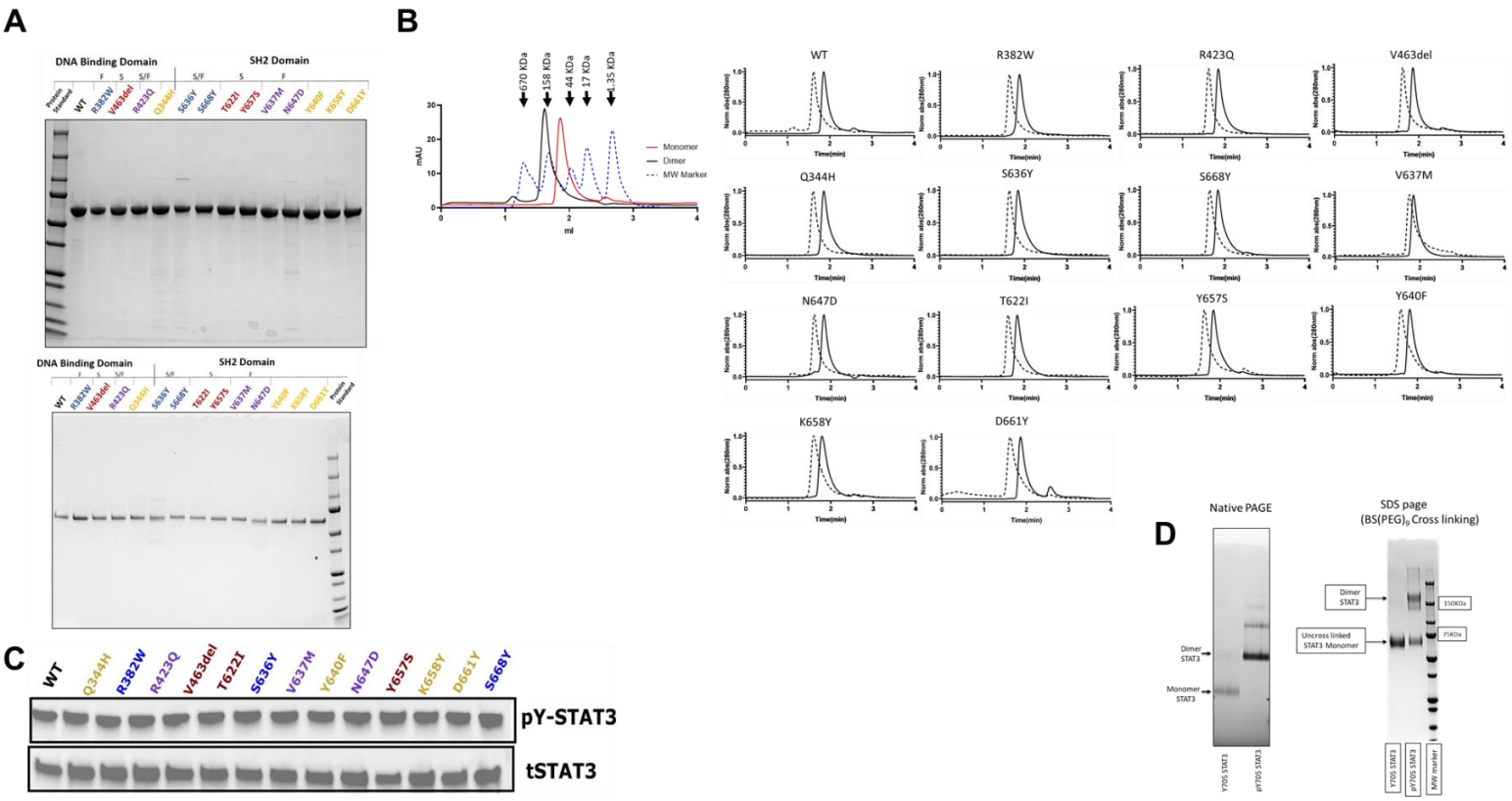

Supplemental Figure 4. Characteristics of bacterially expressed and purified WT and mutant STAT3 proteins. (A) WT and mutant STAT3 proteins were expressed and purified from bacteria and analyzed by SDS-PAGE followed by Coomassie Blue staining and (B) gel filtration. The left panel in B shows the superimposed gel filtration profiles of WT STAT3 protein monomer (red curve), WT STAT3 homodimer (black curve) and protein markers with the indicated molecular weights. The group of panels on the right in B shows the gel filtrations profiles of the purified unphosphorylated (solid line) and phosphorylated (dashed line) of WT and each mutant STAT3 proteins, which demonstrate a single peak of ~70 kDa for the unphosphorylated protein consistent with a monomer in solution and a single peak of ~150 kDa consistent with a homodimer in solution. (C) A representative of three immunoblots of pY-STAT3 proteins purified from BL21 DE3 bacteria developed with antibody to pY-STAT3 and total (t) STAT3, as indicated. (D) Pictures of a native gel (left panel) of WT STAT3 either unphosphorylated or phosphorylated on Y705, as indicated, and an SDS-PAGE gel (right panel) of $BS(PEG)_9$ crosslinked WT STAT3

protein either unphosphorylated or phosphorylated on Y705, as indicated. The sizes of selected molecular weight markers are indicated.

Supplemental Figure 5

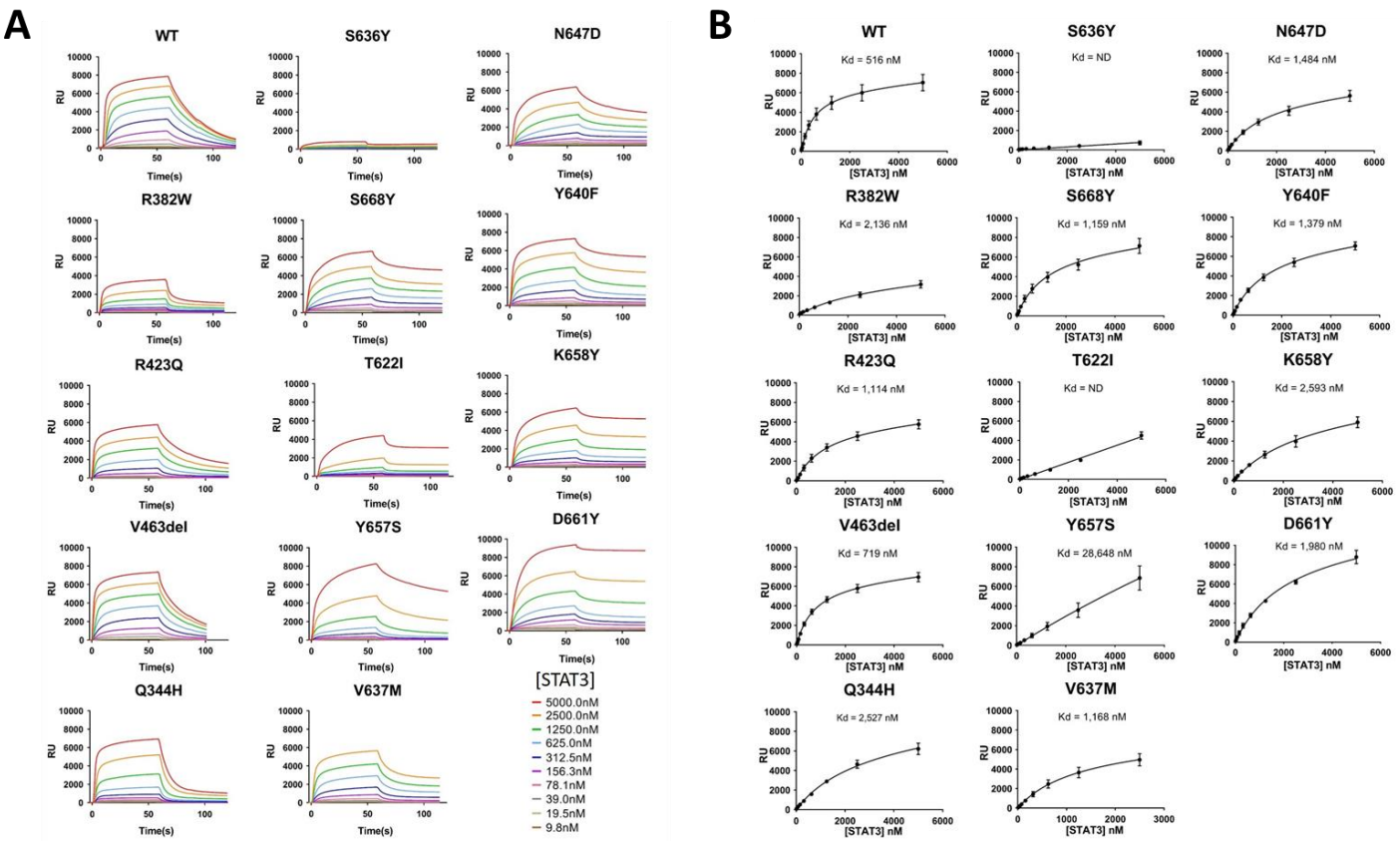

Supplemental Figure 5. Effects of mutations on STAT3 binding to pY1068-peptide. (A) WT or mutant STAT3 protein monomers expressed in bacteria and purified to homogeneity were analyzed for binding to pY1068 or Y1068 dodecapeptide by SPR. Biacore SPR sensograms changes in resonance units (RU) over time show binding to immobilized pY1068-peptide with increasing concentrations of WT or mutant STAT3 protein. (B) Results of steady-state RU changes plotted for each protein as a function of protein concentration; the calculated K_D is shown.

Supplemental Figure 6

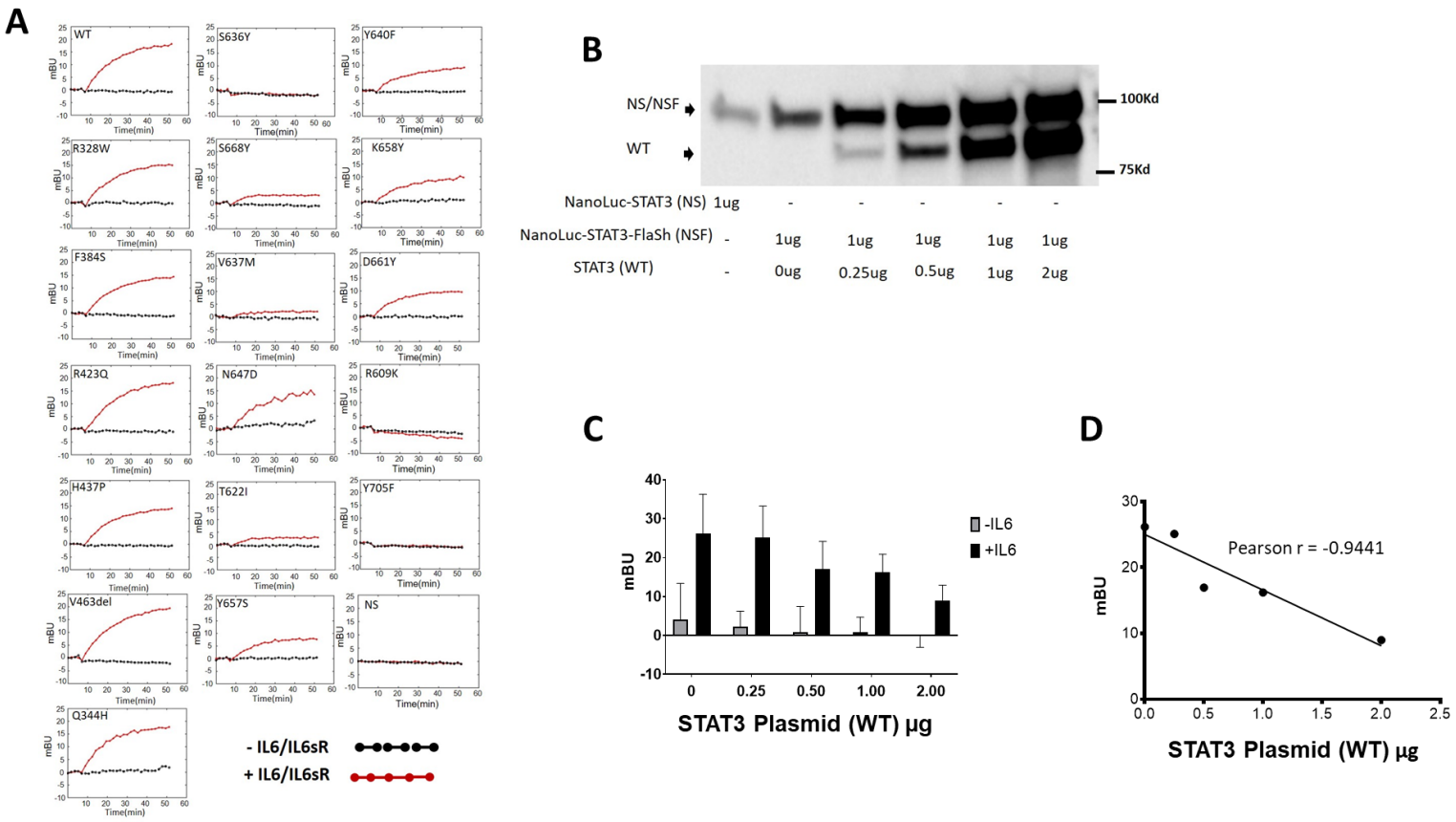

Supplemental Figure 6. Effect of mutations on STAT3 homodimerization assessed using BRET reporter constructs. STAT3 WT and mutant constructs each containing a nano-Luciferase (nLuc) inserted at the N-terminus and a FlAsH motif (NSF) inserted within a flexible loop in the DBD immediately after residue 425 were transiently transfected into MEF$^{-/-}$ cells. (A) Shows BRET measurements of cells assayed for 5 minutes before being incubated without (dashed black line) or with (red line) IL6/sIL6R. Measurements were taken for a duration of 50 minutes. (B) Representative STAT3 immunoblot of protein extracts of MEF$^{-/-}$ cells transiently transfected with the indicated STAT3 constructs; the position of molecular weight markers are indicated. (C) The mean ± SD of fluorescence after 50 minutes of 4 experiments of MEF$^{-/-}$ cells transiently transfected with a constant amount of NSF (1 ug) and increasing amounts of WT STAT3 construct in the presence (black bars) or absence (gray bars) of IL6/sIL6. Pearson's correlation (D) for mBU data as a function of WT STAT3 plasmid amount (ug).

Supplemental Figure 7

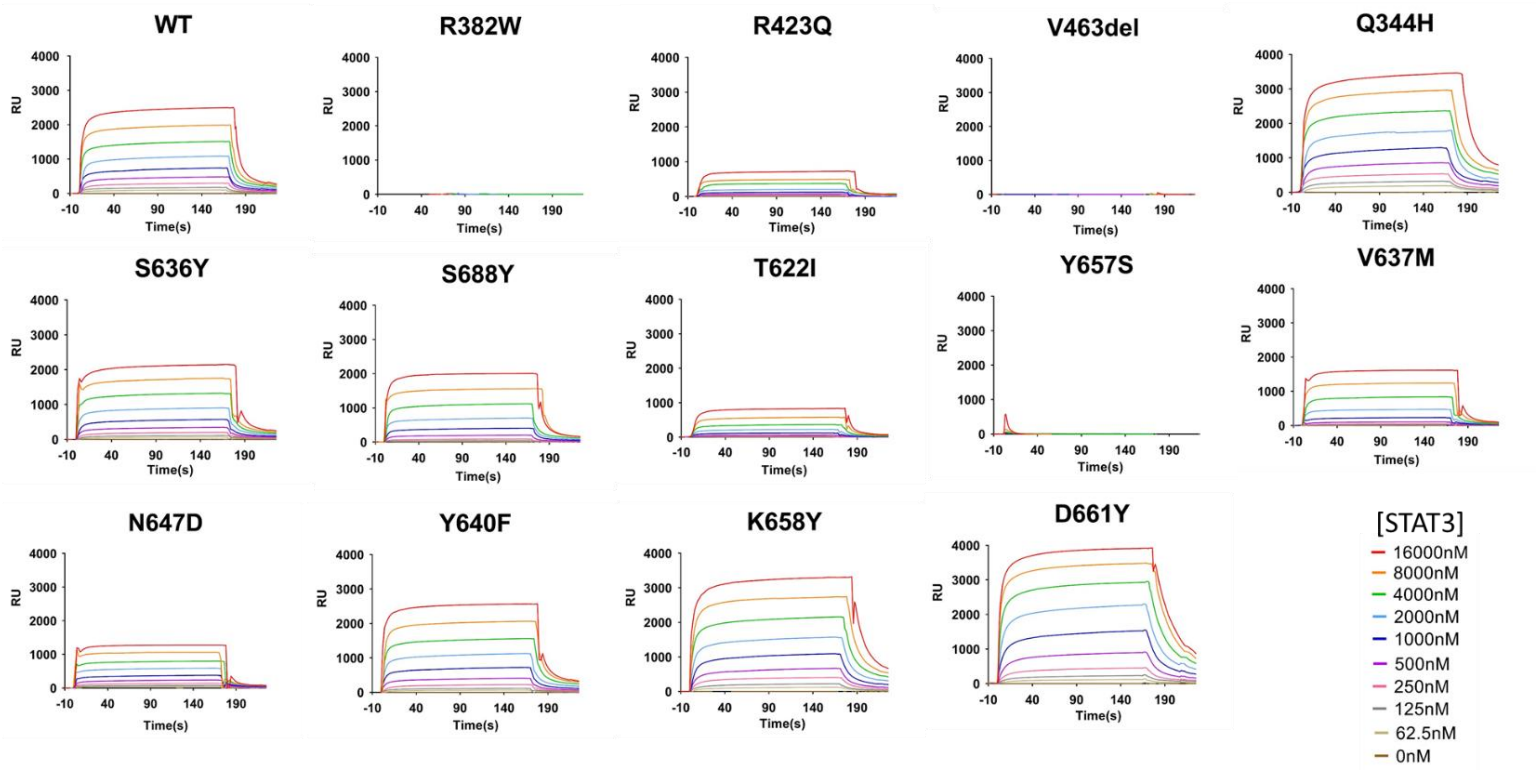

Supplemental Figure 7. Effects of mutations on STAT3 homodimer binding to DNA. WT or mutant pY-STAT3 proteins expressed in bacteria and purified were analyzed for binding to immobilized duplex hSIE DNA by SPR. Sensograms show changes in RU indicative of protein binding to hSIE with increasing concentrations of protein.

Supplemental Figure 8

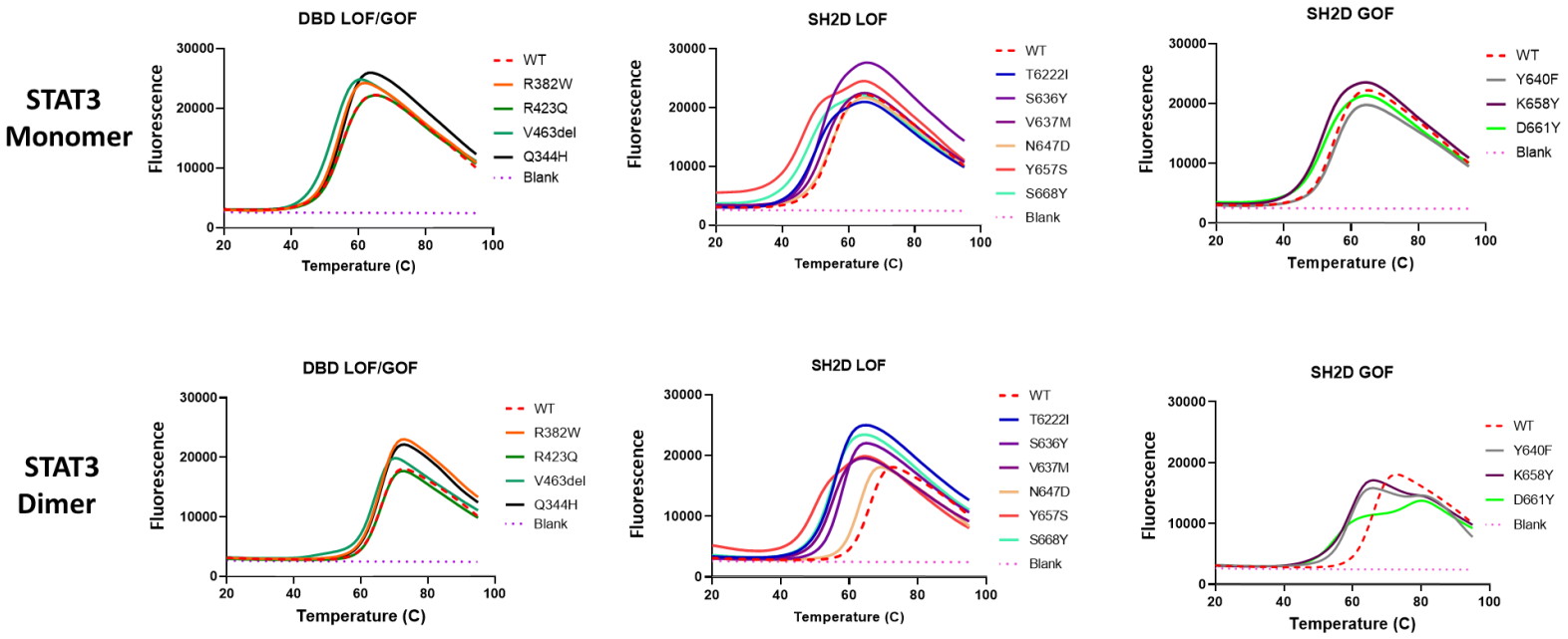

Supplemental Figure 8. Effects of mutations on thermal stability of STAT3 protein monomers and homodimers. Bacterially expressed and purified WT and mutant STAT3 proteins were examined for thermal stability using the DFS assay. Shown is the fluorescence recorded for each WT and mutant STAT3 monomer and homodimer with increasing temperature (heat ramp rate of 0.5°C/min).

Supplemental Figure 9

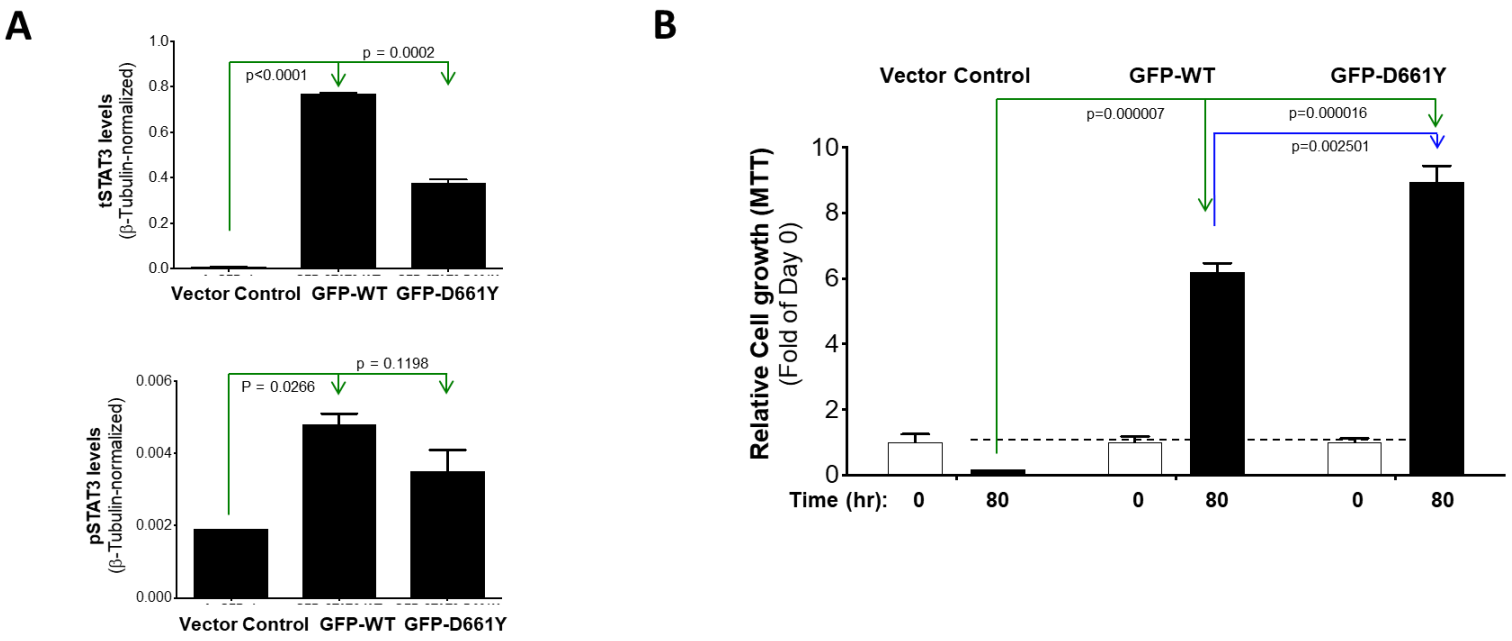

Supplemental Figure 9. Levels of total STAT3 and pY-STAT3 and STAT3-dependent growth of MEF$^{-/-}$ cells following stable transfection with WT STAT3 or with SH2D GOF STAT3 mutant constructs. (A) Levels of total (t) STAT3 and pY-STAT3 normalized to β-tubulin in extracts of MEF$^{-/-}$ cells stably transfected with the indicated constructs. (B) Cell growth was determined after incubation for 80 hours in medium containing 0.5% FBS; data presented are mean ± SD of two independent experiments; p values shown were determined using the two-tailed independent t-test.

Supplemental Figure 10

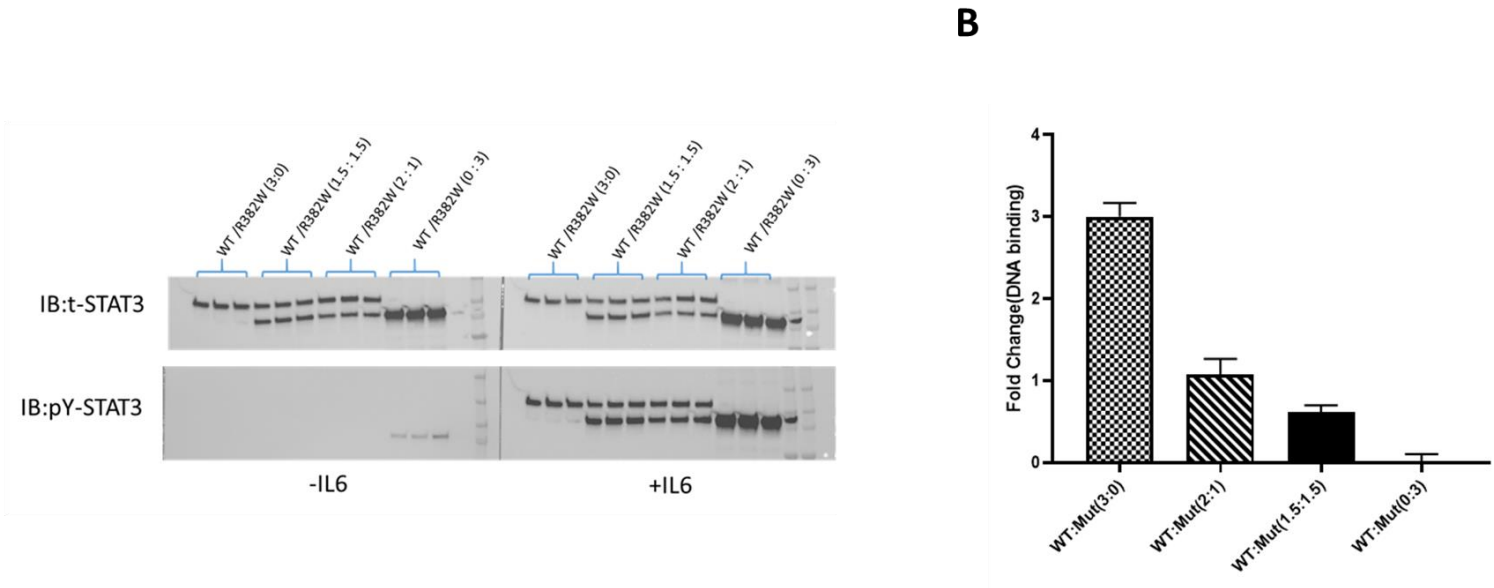

Supplemental Figure 10. Dominant negative effect of STAT3 DBD LOF mutation R382W on DNA binding. A) STAT3$^{-/-}$ MEF cells were transiently transfected with the AcGFP1 WT STAT3 construct or the untagged DBD LOF mutation R382W construct at the indicated weight ratios and incubated without (-) or with (+) IL6/sIL6R. Lysates were separated by SDS-PAGE and immunoblotted (IB) with antibody to pY-STAT3 or total (t) STAT3, as indicated. Representative immunoblots are shown. (B) Lysates were examined for DNA binding using the TransAM STAT3 kit; the value obtained from lysates of stimulated cells was divided by value obtained from lysates of unstimulated cells to obtain the fold increase in DNA binding.

Supplemental Figure 11

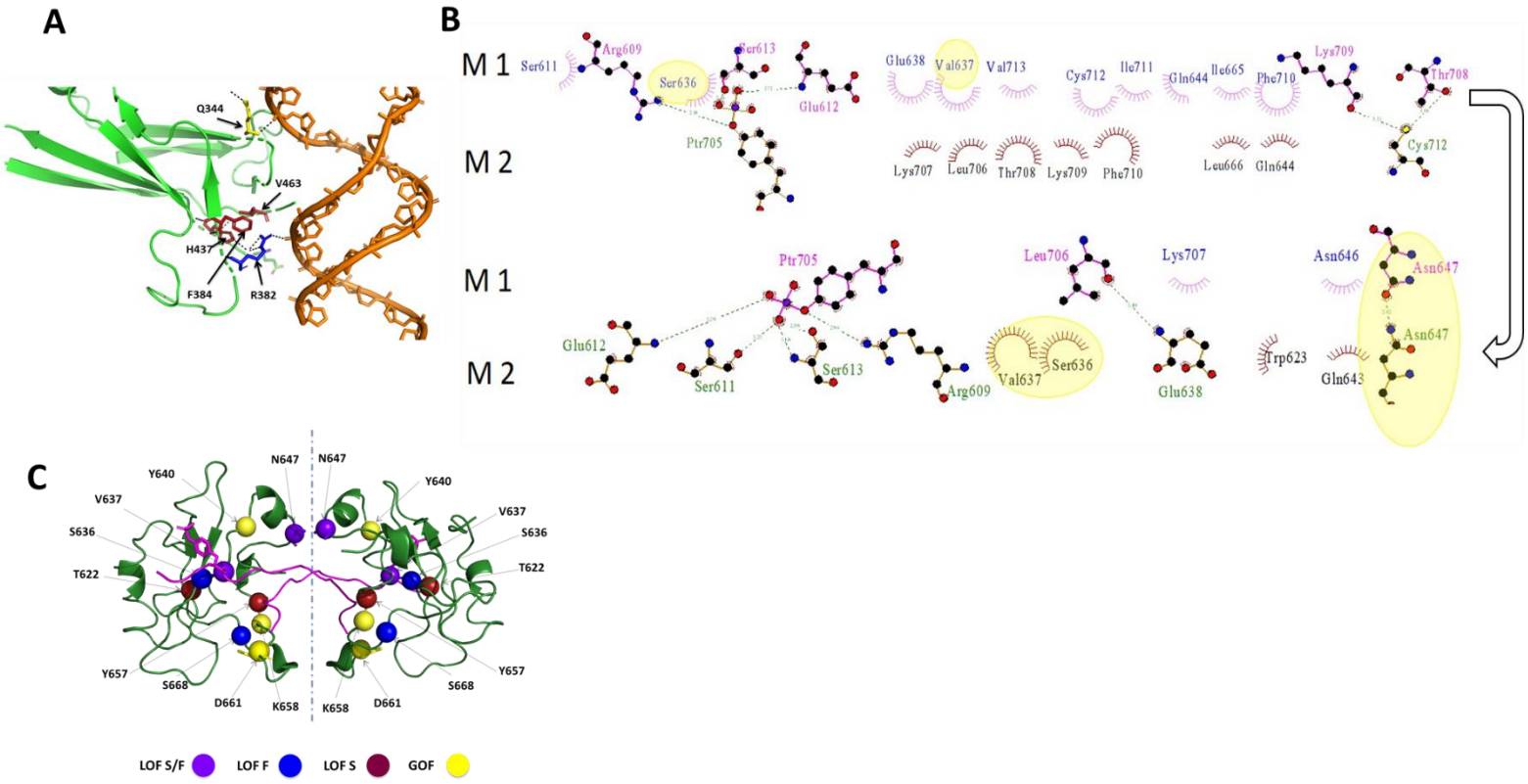

Supplemental Figure 11. Key structural features of STAT3 binding to DNA and homodimer formation. (A) Ribbon diagram depicts the structure of the complex of STAT3 homodimer bound to duplex DNA (1bg1) showing the location and interactions of duplex DNA with key residues within the STAT3 DBD examined in this study (Note: R423Q is not visible on the crystal structure). (B) Dimplot depiction of STAT3 residues within each monomer (M1 and M2) that directly contribute to homodimer formation. Highlighted in yellow are residues mutated in AD-HIES included in this study. S636 and V637 are located within the pY-peptide binding site and interact with pY705 loop. Ribbon diagram (C) of the crystal structure STAT3 homodimer bound to duplex DNA (1bg1) showing the location of residues mutated for this study.

Supplemental Figure 12

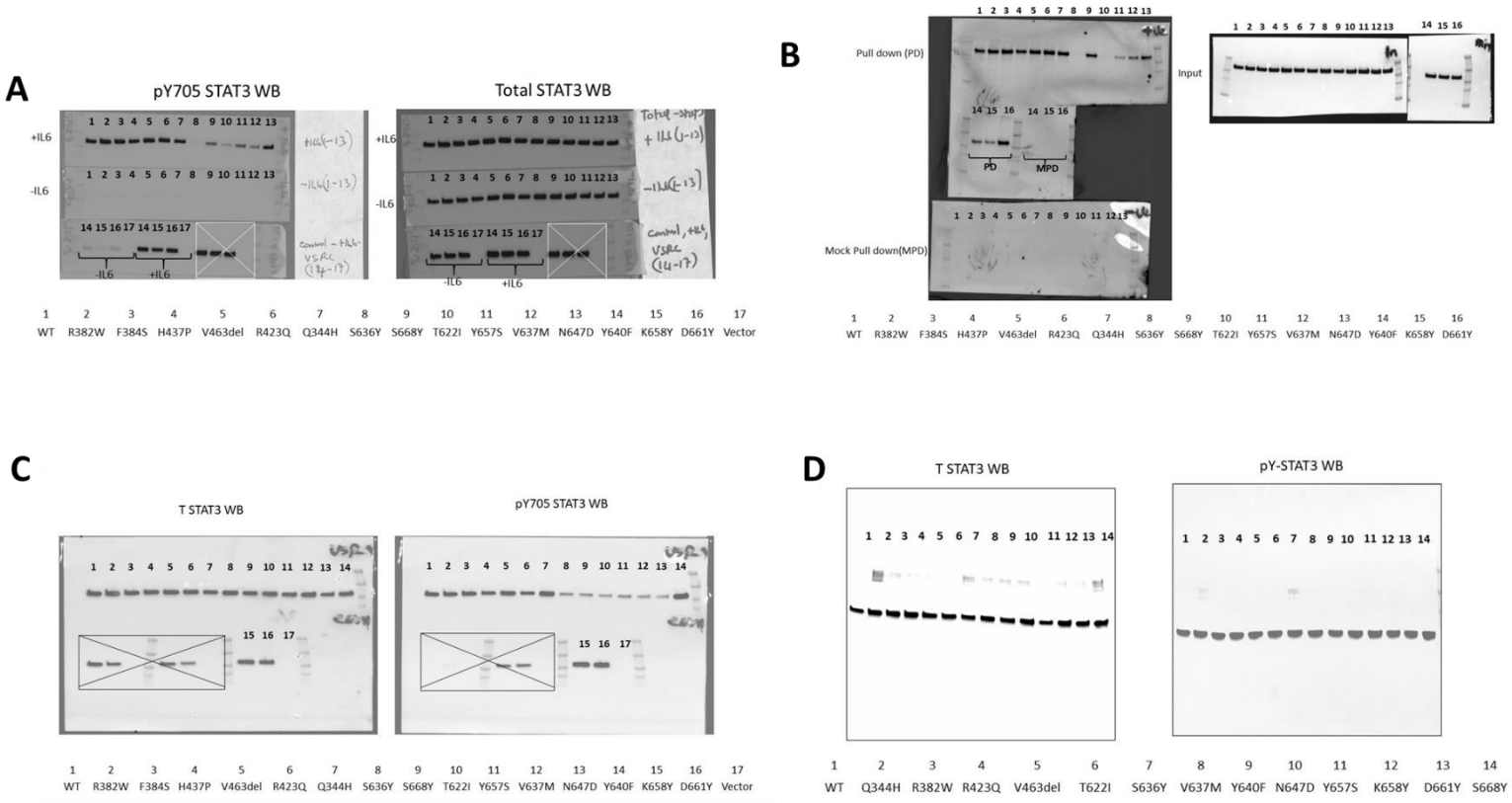

Supplemental Figure 12. Original uncropped images used in the manuscript. Uncropped immunoblot images are shown that correspond to (A) Figure 2A, (B) Figure 3A, (C) Supplemental Figure 2B, and (D) Supplemental Figure 3C.

Supplemental Table 1. STAT3 mutations studied in this work.

STAT3 Mutation	Designation	Reference	Disease
Q344H	GOF	[1]	Lymphoproliferation, autoimmunity
R382W	LOF	[2-4]	AD-HIES
F384S	LOF	[5]	AD-HIES
R423Q	LOF	[3,4]	AD-HIES
H437P	LOF	[6]	AD-HIES
V463del	LOF	[2-4]	AD-HIES
T622I	LOF	[3,4]	AD-HIES
S636Y	LOF	[4]	AD-HIES
V637M	LOF	[4,7]	AD-HIES
Y640F	GOF	[8-11]	T-LGL, NK-LGL, PTCL
N647D	LOF	[12]	AD-HIES
Y657F	LOF	[3]	AD-HIES
K658Y	GOF	[13]	IHCA
D661Y	GOF	[8-11]	T-LCL,NK-LCL,ALCL
S668Y	LOF	[14]	AD-HIES

1. Milner JD, Vogel TP, Forbes L, et al. Early-onset lymphoproliferation and autoimmunity caused by germline STAT3 gain-of-function mutations. *Blood*. 2015;125(4):591-599.
2. Minegishi Y, Saito M, Tsuchiya S, et al. Dominant-negative mutations in the DNA-binding domain of STAT3 cause hyper-IgE syndrome. *Nature*. 2007;448(7157):1058-1062.
3. Bocchini CE, Nahmod K, Katsonis P, et al. Protein stabilization improves STAT3 function in autosomal dominant hyper-IgE syndrome. *Blood*. 2016;128(26):3061-3072.
4. Woellner C, Gertz EM, Schäffer AA, et al. Mutations in STAT3 and diagnostic guidelines for hyper-IgE syndrome. *J Allergy Clin Immunol*. 2010;125(2):424-432.e428.
5. Holland SM, DeLeo FR, Elloumi HZ, et al. STAT3 mutations in the hyper-IgE syndrome. *N Engl J Med*. 2007;357(16):1608-1619.
6. Ma CS, Chew GY, Simpson N, et al. Deficiency of Th17 cells in hyper IgE syndrome due to mutations in STAT3. *J Exp Med*. 2008;205(7):1551-1557.
7. Jiao H, Tóth B, Erdos M, et al. Novel and recurrent STAT3 mutations in hyper-IgE syndrome patients from different ethnic groups. *Mol Immunol*. 2008;46(1):202-206.
8. Couronné L, Scourzic L, Pilati C, et al. STAT3 mutations identified in human hematologic neoplasms induce myeloid malignancies in a mouse bone marrow transplantation model. *Haematologica*. 2013;98(11):1748-1752.
9. Koskela HL, Eldfors S, Ellonen P, et al. Somatic STAT3 mutations in large granular lymphocytic leukemia. *N Engl J Med*. 2012;366(20):1905-1913.
10. Jerez A, Clemente MJ, Makishima H, et al. STAT3 mutations unify the pathogenesis of chronic lymphoproliferative disorders of NK cells and T-cell large granular lymphocyte leukemia. *Blood*. 2012;120(15):3048-3057.
11. Fasan A, Kern W, Grossmann V, Haferlach C, Haferlach T, Schnittger S. STAT3 mutations are highly specific for large granular lymphocytic leukemia. *Leukemia*. 2013;27(7):1598-1600.
12. Chandrasekaran P, Zimmerman O, Paulson M, et al. Distinct mutations at the same positions of STAT3 cause either loss or gain of function. *J Allergy Clin Immunol*. 2016;138(4):1222-1224.e1222.

13. Pilati C, Amessou M, Bihl MP, et al. Somatic mutations activating STAT3 in human inflammatory hepatocellular adenomas. *J Exp Med*. 2011;208(7):1359-1366.
14. Chandesris M-O, Melki I, Natividad A, et al. Autosomal dominant STAT3 deficiency and hyper-IgE syndrome: molecular, cellular, and clinical features from a French national survey. *Medicine*. 2012;91(4):e1-e19.

Supplemental Table 2. Primer Names and Sequence.
STAT3 DNA Probes for SPR

primer name	Primer sequence
FIASH425F	GAATGGGGGCCGAGCCAATTGTTGCCCAGGATGCTGTGTGACTGAGGAGCTGCACCTGATC
FIASH425R	GATCAGGTGCAGCTCCTCAGTCACACAGCATCCTGGGCAACAATTGGCTCGGCCCCCATTC
NI NANOC-A	AAGCAGGCTTGGAAGGAGTTCGAACCATGGTCTTCACACTCGAAGATTTCGTTG
NI NANOB-D	GTGTCAAGCTGCTGTAGCTGATTCCATTGGGCAGCGATCGCGCCGCTCGAGCCCGCCAG
CI NANOC-A	GAGTTGACCTCGGAGTGCGCTACCTCCCCCATGGCATTGGGTAGTTCTGGAGTCTTCACACTCGAAGATTTCGTTG
CI NANOB-D	GTACAAGAAAGCTGGGTTGCGGCCGCACTCGAGCTACGCCAGAATGCGTTCGCACAGCCGCCAGCCGGT
F R609K	CAGGCACCTTCCTGCTAAAATTCAGTGAAAGCAG
R R609K	CTGCTTTCACTGAATTTTAGCAGGAAGGTGCCTG
F Y705F	GTAGCGCTGCCCCATTCCTGAAGACCAAG
R Y705F	CTTGGTCTTCAGGAATGGGGCAGCGCTAC
FOR S668Y	GCTACCAATATCCTGGTGTATCCACTGGTCTATCTCTATC
REV S668Y	GATAGAGATAGACCAGTGGATACACCAGGATATTGGTAGC
FOR S636Y	GCGGTAAGACCCAGATCCAGTACGTGGAACCATACACAAAGC
REV S636Y	GCTTTGTGTATGGTTCCACGTACTGGATCTGGGTCTTACCGC
FOR-D661Y	CATGGGCTATAAGATCATG TAT GCTACCAATATCCTGGTGTC
REV-D661Y	GACACCAGGATATTGGTAGC ATA CATGATCTTATAGCCCATG
FOR-K658Y	GAAATCATCATGGGCTAT TAT ATCATGGATGCTACCAATATC
REV-K658Y	GATATTGGTAGCATCCATGAT ATA ATAGCCCATGATGATTTC
FOR-Y640F	GATCCAGTCCGTGGAACCA TTC ACAAAGCAGCAGCTGAAC
REV-Y640F	GTTCAGCTGCTGCTTTGT GAA TGGTTCCACGGACTGGATC
F Q344H	GACCGGCGTCCACTTCACTACT
R Q344H	AGTAGTGAAGTGGACGCCGGTC
F 384S	TCCCGGAAATCTAACATTCTG
R 384S	CAGAATGTTAGATTTCCGGGA
F R382W	CAGAGGATCCTGGAAATTTAACATTC
R R382W	GAATGTTAAATTTCCAGGATCCTCTG
F H437P	CTGAGGAGCTGCCCCTGATCACC
R H437P	GGTGATCAGGGGCAGCTCCTCAG
F V463d	CTCCTTGCCAGTTGTGATCTCCAACATCTGTC
R V463d	GACAGATGTTGGAGATCACAACTGGCAAGGAG
F T622I	GCGTCACTTTCATTTGGGTGGAGAAG
R T622I	CTTCTCCACCCAAATGAAAGTGACGC
F Y657S	CATCATGGGCTCTAAGATCATGGATG
R Y657S	CATCCATGATCTTAGAGCCCATGATG

hSIE DNA : Biotin - GATCCTTCT GGG AAT TCC TAG ATC TCTC GAT CTA GGA ATT CCC AGA AGG ATC

Mutant hSIE DNA: Biotin - GATCCTTCT GGG CCG TCC TAG ATC TCTC GAT CTA GGA CGG CCC AGA **AGG ATC**

STAT3 peptides for SPR

P1068 Biotin-Ahx-LPVPE{pY}INQSVP-OH

1068 Biotin-Ahx-LPVPEYINQSVP-OH

Supplemental Table 2. Primer Names and Sequence.
STAT3 DNA Probes for SPR

primer name	Primer sequence
FIASH425F	GAATGGGGGCCGAGCCAATTGTTGCCCAGGATGCTGTGTGACTGAGGAGCTGCACCTGATC
FIASH425R	GATCAGGTGCAGCTCCTCAGTCACACAGCATCCTGGGCAACAATTGGCTCGGCCCCCATTC
NI NANOC-A	AAGCAGGCTTGGAAGGAGTTCGAACCATGGTCTTCACACTCGAAGATTTCGTTG
NI NANOB-D	GTGTCAAGCTGCTGTAGCTGATTCCATTGGGCAGCGATCGCGCCGCTCGAGCCCGCCAG
CI NANOC-A	GAGTTGACCTCGGAGTGCGCTACCTCCCCCATGGCATTGGGTAGTTCTGGAGTCTTCACACTCGAAGATTTCGTTG
CI NANOB-D	GTACAAGAAAGCTGGGTTGCGGCCGCACTCGAGCTACGCCAGAATGCGTTCGCACAGCCGCCAGCCGGT
F R609K	CAGGCACCTTCCTGCTAAAATTCAGTGAAAGCAG
R R609K	CTGCTTTCACTGAATTTTAGCAGGAAGGTGCCTG
F Y705F	GTAGCGCTGCCCCATTCCTGAAGACCAAG
R Y705F	CTTGGTCTTCAGGAATGGGGCAGCGCTAC
FOR S668Y	GCTACCAATATCCTGGTGTATCCACTGGTCTATCTCTATC
REV S668Y	GATAGAGATAGACCAGTGGATACACCAGGATATTGGTAGC
FOR S636Y	GCGGTAAGACCCAGATCCAGTACGTGGAACCATACACAAAGC
REV S636Y	GCTTTGTGTATGGTTCCACGTACTGGATCTGGGTCTTACCGC
FOR-D661Y	CATGGGCTATAAGATCATG TAT GCTACCAATATCCTGGTGTC
REV-D661Y	GACACCAGGATATTGGTAGC ATA CATGATCTTATAGCCCATG
FOR-K658Y	GAAATCATCATGGGCTAT TAT ATCATGGATGCTACCAATATC
REV-K658Y	GATATTGGTAGCATCCATGAT ATA ATAGCCCATGATGATTTC
FOR-Y640F	GATCCAGTCCGTGGAACCA TTC ACAAAGCAGCAGCTGAAC
REV-Y640F	GTTCAGCTGCTGCTTTGT GAA TGGTTCCACGGACTGGATC
F Q344H	GACCGGCGTCCACTTCACTACT
R Q344H	AGTAGTGAAGTGGACGCCGGTC
F 384S	TCCCGGAAATCTAACATTCTG
R 384S	CAGAATGTTAGATTTCCGGGA
F R382W	CAGAGGATCCTGGAAATTTAACATTC
R R382W	GAATGTTAAATTTCCAGGATCCTCTG
F H437P	CTGAGGAGCTGCCCCTGATCACC
R H437P	GGTGATCAGGGGCAGCTCCTCAG
F V463d	CTCCTTGCCAGTTGTGATCTCCAACATCTGTC
R V463d	GACAGATGTTGGAGATCACAACTGGCAAGGAG
F T622I	GCGTCACTTTCATTTGGGTGGAGAAG
R T622I	CTTCTCCACCCAAATGAAAGTGACGC
F Y657S	CATCATGGGCTCTAAGATCATGGATG
R Y657S	CATCCATGATCTTAGAGCCCATGATG

hSIE DNA : Biotin - GATCCTTCT GGG AAT TCC TAG ATC TCTC GAT CTA GGA ATT CCC AGA AGG ATC

Mutant hSIE DNA: Biotin - GATCCTTCT GGG CCG TCC TAG ATC TCTC GAT CTA GGA CGG CCC AGA **AGG ATC**

STAT3 peptides for SPR

P1068 Biotin-Ahx-LPVPE{pY}INQSVP-OH

1068 Biotin-Ahx-LPVPEYINQSVP-OH